

Adaptive l_0 -LMS based algorithm for solution of power quality problems in PV-STATCOM based system

Nimita A. Gajjar¹, Tejas Zaveri², Naimish Zaveri²

¹Department of Electrical Engineering, Dr. S and S.S Ghandhy Government Engineering College, Gujarat Technological University, Gujarat, India

²Department of Electrical Engineering, C.K Pithawalla College of Engineering and Technology, Gujarat Technological University, Gujarat, India

Article Info

Article history:

Received May 31, 2022

Revised Aug 13, 2022

Accepted Sep 30, 2022

Keywords:

Adaptive control

DSTATCOM

Smart inverter

Unity power factor operation

Voltage control

ABSTRACT

This paper presents grid tied photovoltaic-static synchronous compensators (PV-STATCOM) system using an adaptive l_0 -LMS based control algorithm. The proposed l_0 -LMS with adaptive zero attractor is used for single stage grid connected PV-STATCOM system and it highlights the performance of system for maintaining unity power factor, reducing harmonics and zero voltage regulation with nonlinear and unbalanced load. In this the l_0 norm constraint least means square (LMS) algorithm, the optimal value of zero attractor is time varying instead of a fixed value such that it gives better results with variable input systems such as PV power. The system is tested on a low cost prototype developed using STM32F407VG microcontroller and the results are found satisfactory.

This is an open access article under the [CC BY-SA](#) license.



Corresponding Author:

Nimita Gajjar

Department of Electrical Engineering, Dr. S and S.S Ghandhy Government Engineering College

Gujarat Technological University

Gujarat, India

Email: nimita_gajjar@hotmail.com

1. INTRODUCTION

Distributed generation like solar, wind, mini hydro, and hybrids are gaining popularity in remote locations owing to the fact that it needs no transmission lines, is less polluting, and is efficient and economic. A solar photovoltaic (SPV) system provides clean power to consumers at a low rate and moderate efficiency. With the increase in connection of SPV systems into the grid, it also gives rise to certain limitations, like steady state and temporary overvoltage, power fluctuations, harmonics, and other power quality (PQ) issues. These PQ issues have been taken care of by power electronic converters such as distribution static compensator (DSTATCOM). The DSTATCOM acts as a shunt connected active power filter, which provides reactive power compensation as well as harmonic reduction [1]. The PV inverter itself will act as a DSTATCOM and hence increase the utilisation of the switches by two fold, which otherwise would remain idle in the absence of PV power. Several control strategies for reference current generation and configuration of DSTATCOM are reported in various literature. Various maximum power point tracker (MPPT) algorithms for maximum power extraction that can be possible from PV arrays under variable solar insolation are also reported in [2]-[4]. Adaptive algorithms based on adaptive linear neuron (ADALINE) least means square (LMS) and variations on LMS, such as least means forth (LMF), combined LMS-LMF, recursive LMS, and VLG-LMS, have gained prominence over conventional control algorithms such as synchronous reference frame theory (SRF), instantaneous reactive power theory (IRPT), and SCT as they provide fast response

under variable input conditions such as solar and wind. Godavarti and Hero [5] presents the technique for updation of the parameters in the LMS filter in a manner that reduces the computational burden. Kohli and Mehra [6] discussed the analysis of MG-LMS two-step algorithms under time-varying conditions. The setting of smoothing and control parameters improves tracking performance and stability. Authors have shown a reduced complexity filtered-s LMS (FSLMS) algorithm for controlling non-linear noise [7]. References in [8]-[10] used a different variant of LMS algorithm in which the regularisation parameter is updated dynamically and in [11], fast fourier transform (FFT) and fast hartley transform (FHT) is employed for reducing computational complexity. Giri *et al.* [12]-[14] demonstrate variation in the basic LMS algorithm to increase system dynamic response and to adapt to variable input conditions. Research by Agarwal *et al.* [15], the learning loss mitigation funding (LLMF) theory is proposed in which a leakage factor is introduced to alleviate stalling and stability system response. Khan *et al.* [16] proposed the least-mean-sixth algorithm for PQ mitigation. The Kalman filter approach is discussed in [17]. Harris hawk optimization technique is proposed in [18]. The four-wire multilevel configuration is discussed in [19]. Performance of QLMS approach for abnormal condition is discussed in [20]. In the presented work, a zero attractor is included for updating the tap weight vector, and a l_0 norm driven tap vector constraint is incorporated in cost function of LMS, thus enhancing the convergence speed. The adaptive zero attractor is selected in l_0 norm constraint LMS (l_0 -LMS) algorithm and the optimal value for each iteration is derived by reducing transient mean square deviation. The performance of the PV-DSTATCOM system is observed for active power transfer from PV to grid, reactive power as required by load, mitigating PQ challenges like harmonics, unity power factor operation, and voltage control for nonlinear and unbalanced load conditions. This algorithm is established in the signal-processing domain, and the results of its implementation for addressing PQ issues are found satisfactory. The adaptive l_0 -LMS algorithm is utilised here to solve PQ concerns such as low power factor and harmonics reduction. The peak power from the PV module is extracted using the incremental conductance (InC) MPPT technology, and the active power is given to the load connected to the point of common interface (PCI) as well as into the grid. The adaptive l_0 -LMS algorithm is used to operate voltage source inverter (VSI) for reactive power compensation and to eradicate harmonics from the system. Also, the system stability is maintained during unbalanced loading conditions. In this paper, section 2 contains the system configuration, a description of control scheme, and different modes of operation. The simulation results of proposed system are reported in section 3. Section 4 discusses the conclusion.

2. METHOD

Figure 1 depicts the proposed system configuration. It comprises a PV array, a three-phase VSI, an interfacing inductor, an RC filter, and a nonlinear load connected at PCC. A single-stage converter topology has been chosen to connect the PV-DSTATCOM system to three-phase grid at PCC. Several MPPT techniques have already been reported in several studies for obtaining peak power from a solar PV array under diverse environmental circumstances [21]-[23]. In comparison to other techniques, an InC algorithm is found to be faster. The peak power from the PV array is extracted by implementing an InC based approach over varying environmental circumstances.

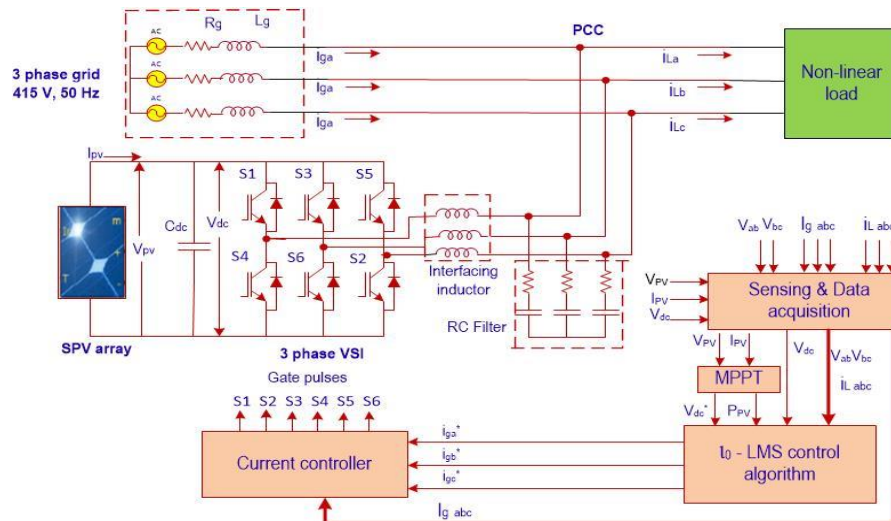


Figure 1. Schematic of the proposed system

2.1. Proposed l_0 -LMS algorithm

In this work l_0 norm constraint LMS algorithm with adaptive zero attractor is presented. Instantaneous values are taken into account in the standard LMS algorithm that might cause slower convergence. In the proposed algorithm, a zero attractor (ZA) term is added, which accelerates the convergence speed by attracting near zero coefficient to zero. However, the performance of l_0 norm is dependent on value of zero attractor term. The setting of a fixed zero attractor is difficult when the system has a time-varying noise signal. We present an adaptive algorithm to select ZA in the l_0 norm. Estimation of weights of real and reactive load current components, real and reactive loss components are the main functions of the AZA l_0 -LMS control algorithm. In addition, templates for in-phase and quadrature units are extracted and reference grid currents are generated. Actual current is then compared with reference in a hysteresis current controller and corresponding gating signals are generated for switching the VSI. Consider the following linear regression model.

$$d(k) = w^T x(k) + v(k) \quad (1)$$

Where $d(k)$ symbolized desired signal, w is unknown impulse response vector, $x(k)$ indicates input vector whereas noise signal is denoted as $v(k)$. In the proposed l_0 -LMS algorithm, the weights are updated as,

$$w(k+1) = w(k) + \mu e(k)x(k) + \rho \xi_0(w(k)) \quad (2)$$

Where $w(k) = [w_0(k), w_1(k), \dots, w_{L-1}(k)]^T$ denotes filter tap weight vector, k represents the time scale, the parameter μ is LMS convergence coefficient or step size of adaptation. The error signal $e(k)$ is calculated as in (3),

$$e(k) = d(k) - w^T(k)x(k) \quad (3)$$

The term $\rho \xi_0(w(k))$ in (2) represents the zero-attraction term, in which the parameter $\rho > 0$ denotes the zero attractor, whereas the term $\xi_0(w(k))$ implies the subgradient of the tap weight penalty in l_0 norm, and the subgradient is specified as in (4) for each entry of $0 \leq i \leq L$,

$$\xi_0(w_i(k)) = \alpha^2 w_i(k) - \alpha sgn(w_i(k)), \leq \frac{1}{\alpha} \quad (4)$$

$$= 0, \text{otherwise}$$

Where the strength as well as range of zero-attraction is governed by positive parameter $\alpha > 0$. With reference to steady state mean square deviation (MSD), the optimum zero attractor is positively connected to noise power (17) in [24]. If there is any change in the level of the signal, the zero attractor resets to improve the steady-state performance of the l_0 -LMS algorithm. We introduce the adaptive zero attractor along with l_0 -LMS algorithm (AZA l_0 -LMS) to improve the ability of the algorithm to adapt to time-varying signals. Based on the objective of minimising transient MSD as much as achievable during the convergence process, we begin by optimising the drop in transient MSD to get the optimum value of zero attractor after every iteration. Then practical values are obtained from the optimal solution. The optimal value of ZA is given as,

$$\rho_{opt} = \frac{E[w^T(k)\xi_0(w(k))] - \mu E[e(k)x^T(k)\xi_0(w(k))]}{E[\xi_0^T w(k)\xi_0(w(k))]} \quad (5)$$

The time averages of all three expectation on RHS of (5) is approximated as,

$$\psi(k+1) = \beta\psi(k) + (1-\beta)w^T(k)\xi_0(w(k)) \quad (6)$$

$$\phi(k+1) = \beta\phi(k) + (1-\beta)x^T(k)\xi_0(w(k)) \quad (7)$$

$$\varPhi(k+1) = \beta\varPhi(k) + (1-\beta)\xi_0^T w(k)\xi_0(w(k)) \quad (8)$$

Where $\psi(k+1)$, $\phi(k+1)$ and $\varPhi(k+1)$ represents the three expectation terms on RHS of (5). Furthermore, the value of smoothing parameter β is chosen to set to near unity for proper time smoothing. In this paper, the value of β is selected at 0.99. The reference optimal ZA is now written as,

$$\rho_{opt}(k+1) = \begin{cases} \frac{\varPhi(k+1) - \mu\phi(k+1)}{\varPhi(k+1)}, & \text{if } \phi(k+1) \neq 0 \\ 0, & \text{if } \phi(k+1) = 0 \end{cases} \quad (9)$$

In case of denominator equals to zero in (9) when $\rho_{opt}(k+1)$ is set to zero the proposed algorithm behaves as standard LMS algorithm. If the elements in tap weight vector is either zero or higher than $1/\alpha$, then there is no pull towards zero on any coefficients and the term $\rho_{opt}(k+1)$ is equal to zero.

2.2. Extraction of active and reactive load current component

Figure 2 represents a detailed diagram of l_0 -LMS based adaptive filter. After each iteration, the active weight components are evaluated and updated. The load current, weight, and input signal are used to determine the error signal. The weights adjust themselves to filter out unwanted harmonics in the load current and provide fundamental component of reference weights. Flowchart for the extraction of components is as shown in Figure 3. The weight vector of active component of a load current of phase ‘a’ is calculated as,

$$w_{pa}(k+1) = w_{pa}(k) + \mu_{pa}e(k)x(k) + \rho\xi_0(w_{pa}(k)) \quad (10)$$

$$e(k) = i(k) - \mu_{pa}(k)w_{pa}(k) \quad (11)$$

In the same manner, active weight vector of load currents in the phases ‘b’ and ‘c’ are calculated as,

$$w_{pb}(k+1) = w_{pb}(k) + \mu_{pb}e(k)x(k) + \rho\xi_0(w_{pb}(k)) \quad (12)$$

$$w_{pc}(k+1) = w_{pc}(k) + \mu_{pc}e(k)x(k) + \rho\xi_0(w_{pc}(k)) \quad (13)$$

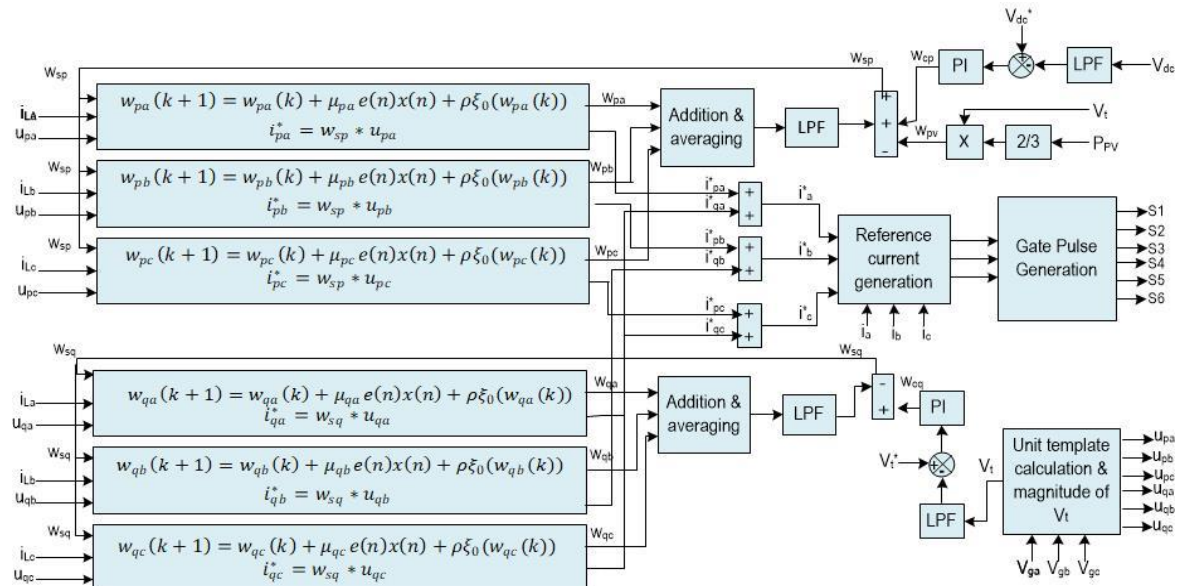


Figure 2. Control structure of the proposed system

Furthermore, the weight vector of reactive component of phase ‘a’ load current is estimated as,

$$w_{qa}(k+1) = w_{qa}(k) + \mu_{qa}e(k)x(k) + \rho\xi_0(w_{qa}(k)) \quad (14)$$

In the same manner, weight vector of reactive components of phases ‘b’ and ‘c’ load currents are calculated as,

$$w_{qb}(k+1) = w_{qb}(k) + \mu_{qb}e(k)x(k) + \rho\xi_0(w_{qb}(k)) \quad (15)$$

$$w_{qc}(k+1) = w_{qc}(k) + \mu_{qc}e(k)x(k) + \rho\xi_0(w_{qc}(k)) \quad (16)$$

2.3. Extraction of active and reactive loss components

Weight of active as well as reactive loss component is given as,

$$w_{cp}(k+1) = w_{cp}(k) + k_p(v_{dc}(k+1) - v_{dc}(k)) + k_i v_{dc}(k+1) \quad (17)$$

$$w_{cq}(k+1) = w_{cq}(k) + k_p(v_t(k+1) - v_t(k)) + k_i v_t(k+1) \quad (18)$$

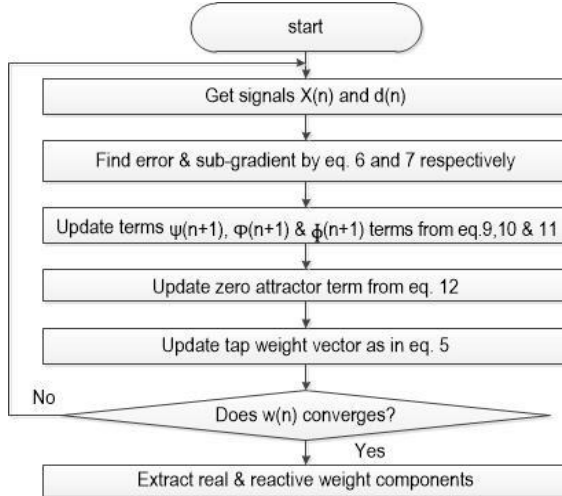


Figure 3. Flowchart of proposed algorithm

2.4. Estimation of unit templates

In phase as well as quadrature unit template can be calculated as,

$$u_{pa} = \frac{v_a}{v_t}, u_{pb} = \frac{v_b}{v_t} \text{ and } u_{pc} = \frac{v_c}{v_t} \quad (19)$$

$$\text{Where } v_t = \sqrt{\frac{2}{3}(v_a^2 + v_b^2 + v_c^2)} \quad (20)$$

$$u_{qa} = \frac{u_{pb}-u_{pc}}{\sqrt{3}}, u_{qb} = \frac{\sqrt{3}u_{pa}}{2} + \frac{u_{pb}+u_{pc}}{2\sqrt{3}} \text{ and } u_{qc} = \frac{-\sqrt{3}u_{pa}}{2} + \frac{u_{pb}-u_{pc}}{2\sqrt{3}} \quad (21)$$

2.5. Generation of reference current

The weight vectors are averaged to determine the equivalent weight for active and reactive component of current. The averaging of weight vector aids in minimizing any imbalance in the current components. The total active weight vector w_{Tp} and reactive weight w_{Tq} of grid current reference can be given as,

$$w_{Tp} = w_{Lpa} + w_{cp} \quad (22)$$

Where w_{Lpa} is total average active component of load current and w_{cp} is active loss component,

$$w_{Tq} = w_{cq} - w_{Lqa} \quad (23)$$

Where w_{Lqa} is total average reactive component of load current and w_{cq} is reactive loss component,

3. RESULTS AND DISCUSSION

The proposed system as well as adaptive LMS based algorithm is developed and simulated in MATLAB Simulink software using the simpower system (SPS) toolbox for simulation. The SPV array is designed for a maximum power output of 7.5 kW, and the PV inverter is rated at 7.5 KVA. The simulation of SPV array is as per [25] Also, the design of its various components is carried out in detail, such as value of the DC bus voltage and capacitor, the interface inductance, and the ripple filter. Under nonlinear operating conditions (balanced and unbalanced) and variable solar irradiance, the performance of the presented system is simulated. Various simulation parameters are as in Table 1.

Table 1. Simulation parameters

Parameter	Value
LMS convergence coefficient μ	5e-3
ZA strength and range α	1e5
Smoothing parameter β	0.99
Carrier frequency	10 KHz

3.1. Simulation results

3.1.1. Performance of the system operating to support unity power factor (.)

The proposed l_0 -LMS control algorithm is simulated for non-linear unbalanced load condition. The unbalanced condition is created by disconnecting load in phase C at 0.5s and its effects on source current, source voltage and compensator current waveforms are observed. As shown in Figures 4(a) and (b) the PV inverter is supplying extracted PV power to the connected load and or grid as well as acting as DSTATCOM compensating harmonics injected into the system by non-linear load and trying to maintain sinusoidal grid currents. The active and reactive both powers will be supplied from PV array. The DC link voltage and PCC voltages are also maintained constant. Figure 4(c) also shows various internal control signals.

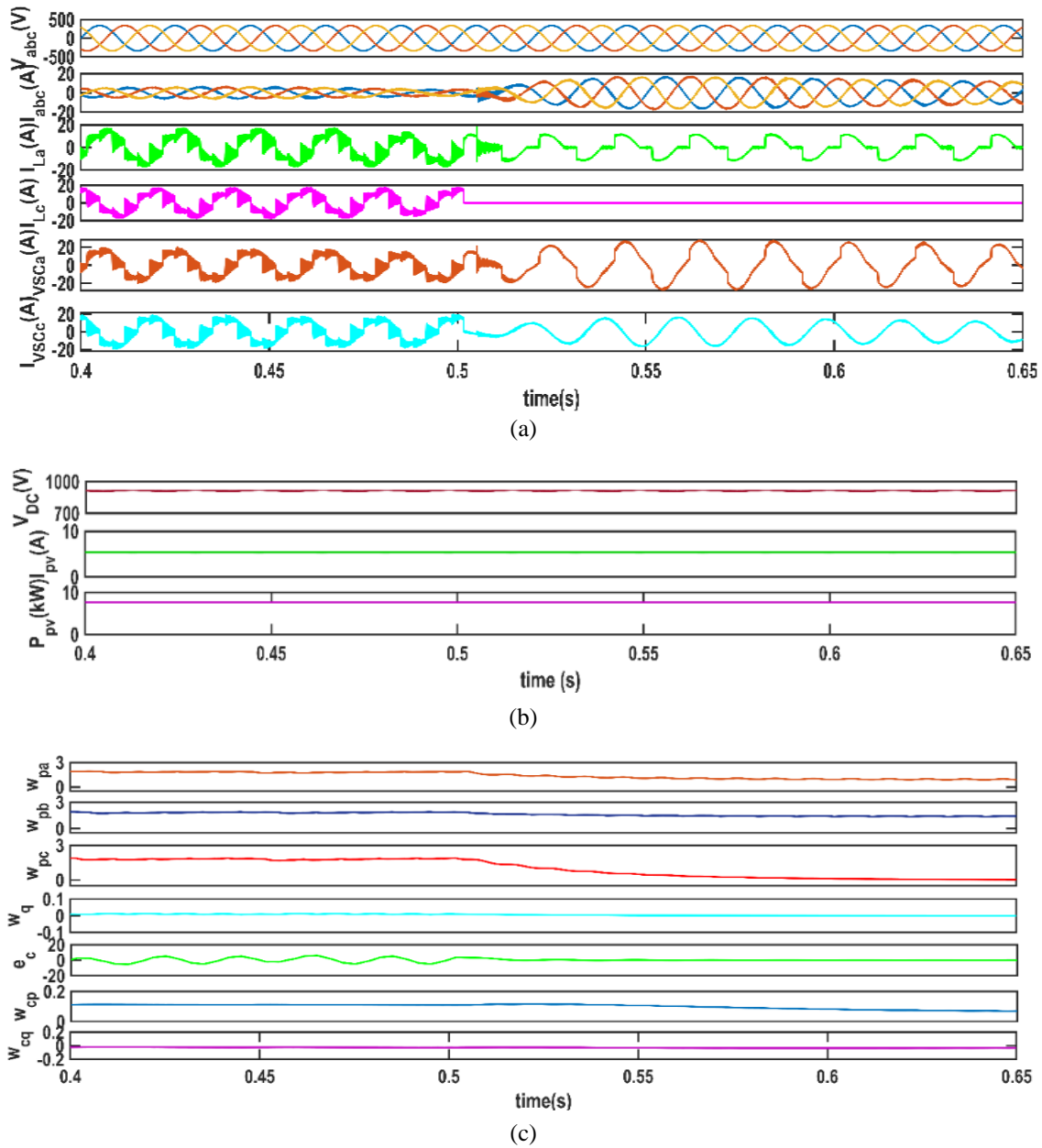


Figure 4. Performance of the system under unbalance non-linear load for maintaining power factor (a) V_{abc} , I_{abc} , load current (a and c phase), converter current (a and c phase), (b) V_{dc} , I_{pv} and P_{pv} , and (c) intermediate control signals

3.1.2. Performance of the system operating to support ZVR mode

The inverter has the capacity to exchange both active and reactive power. It utilizes the remaining capacity of inverter after active power exchange. In addition, when PV power is not available (either due to

whether conditions or in nighttime), the PV inverter will now utilise as active filter to support required reactive power. Grid is supplying active power and grid current is maintain sinusoidal as PV inverter now manages reactive power. Figures 5(a) and (b) shows dynamic performance of the system when operating under ZVR mode.

3.1.3. System dynamics with variable solar irradiance

The behaviour of the system for variable solar insolation is as shown in Figure 5(c). At 0.15 s, the solar irradiance is increased from 500 W/m^2 to 800 W/m^2 . The maximum power is extracted from SPV array by MPPT algorithm and the extracted power is supplied to the load as well as grid. After increase in PV power the grid current increases, slightly as more power is now injected into the grid. Load is maintained constant so surplus power is injected into the grid and active grid power is negative indicating reverse power flow into the grid. The harmonic spectrum of grid current and load current is compared in Figures 6(a) and (b).

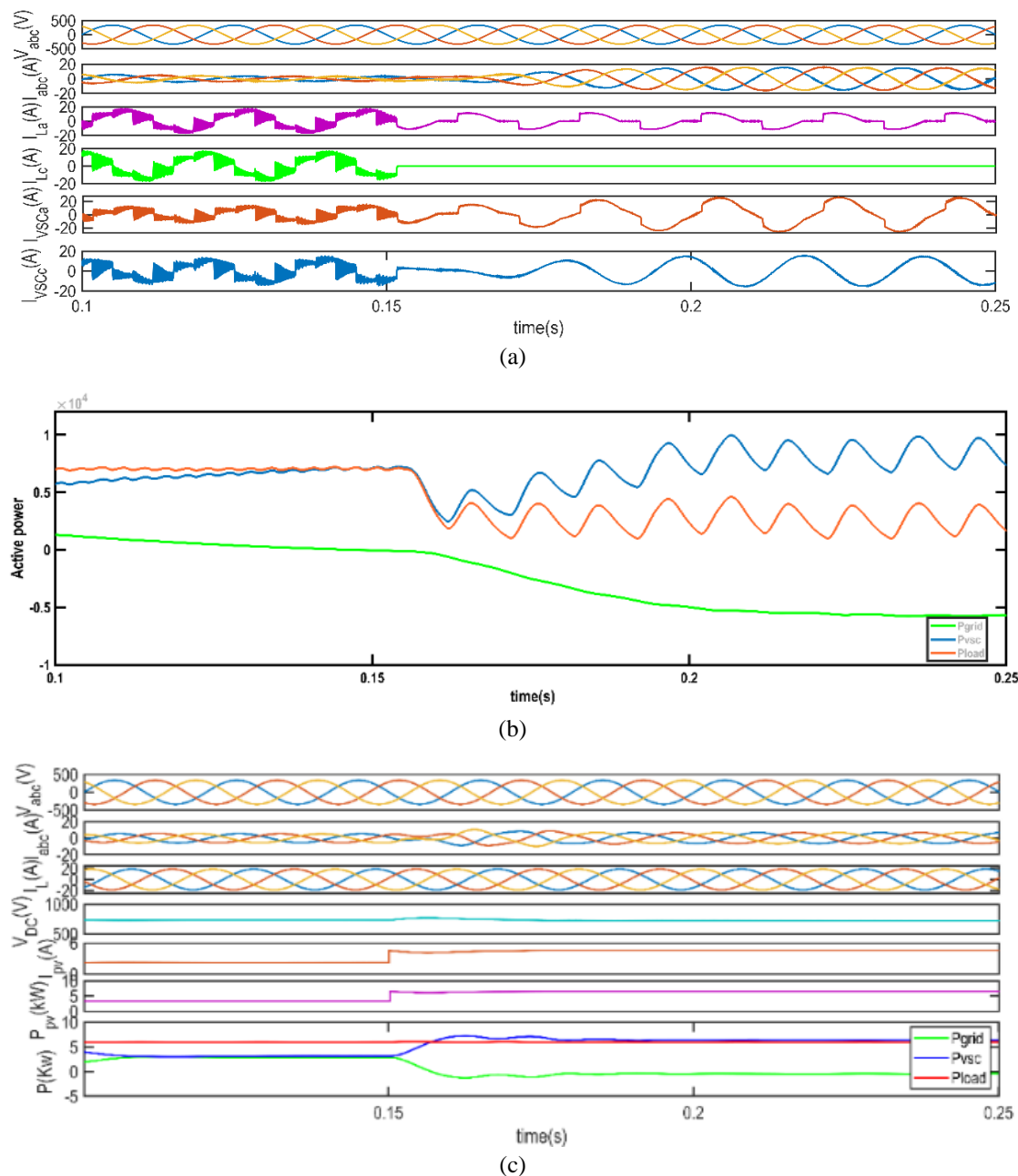


Figure 5. System performance under various operating modes (a) dynamic performance under ZVR mode, (b) Active power distribution under ZVR mode, and (c) system performance under variable PV power

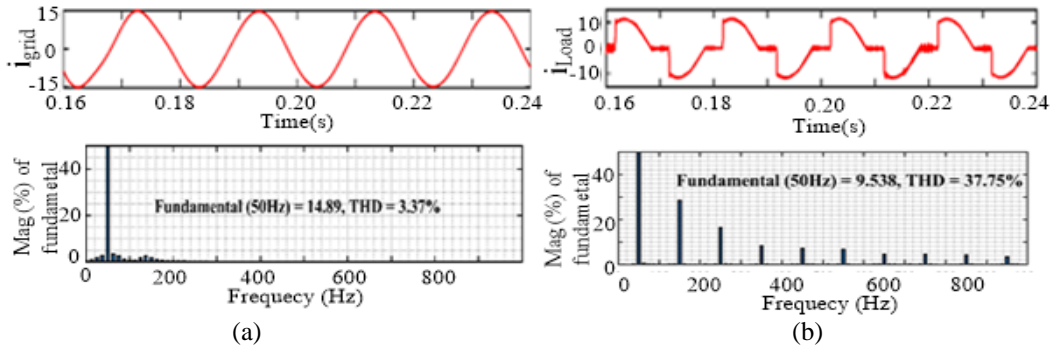
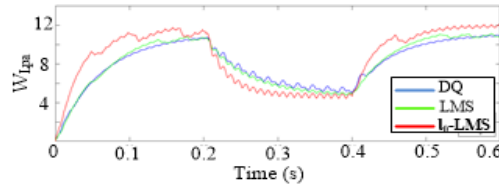


Figure 6. Harmonic spectrum (a) source current and (b) load current with non-linear load

3.1.4. Performance comparison of proposed algorithm with dq and LMS algorithm

The proposed l_0 -LMS control algorithm is compared with dq and LMS algorithm as shown in Figure 7. It is observed that the settling time is less for l_0 -LMS algorithm as compared to other algorithms under consideration. The value of the fundamental active component extracted during unbalanced load conditions by l_0 -LMS is more accurate than dq and LMS algorithm for same condition. Total harmonic distortion (THD) for all three algorithms is as shown in Table 2. THD is 3.8%, 4.1% and 3.37% for dq, LMS and l_0 -LMS algorithms respectively.

Figure 7. Performance comparison of dq, LMS and l_0 -LMSTable 2. Comparison of various parameters for dq, LMS and l_0 -LMS algorithm

Performance parameter	DQ	LMS	l_0 -LMS
THD	3.8%	4.1%	3.37%
Complexity	Less	Medium	Medium
Settling time	0.18s	0.17s	0.1s
Accuracy	Good	Good	Better
No. of computation	Medium	Less	Less
Oscillation	Medium	High	Slightly less

3.2. Laboratory setup

A prototype of the proposed system is developed in the laboratory, and it is tested for various conditions as shown in Figure 8. An autotransformer is used to step down 400 V, 50 Hz, three-phase grid voltage to 110 V. A 6 mH inductor is connected to 110 V for realising the transmission line. Six PV arrays (WAREE make, each of 150 Wp) are connected in series for 900 Wp output. Switching frequency ripples are reduced by an RC filter connected after the three-phase H bridge inverter. Hall effect voltage/current sensors (NITECH made) are used for sensing various quantities like DC voltage, grid voltage, and grid/load/PV currents [23]. The proposed adaptive l_0 -LMS for reference current generation is implemented using ARM-CORTEX M4 microcontroller (STM32F407VG). For recording the performances of the proposed system, a four-channel DSO (Agilent make) is used. The system is tested under various conditions and the results are presented as below. The hardware results for various conditions are as shown in Figure 9. The system is first tested for only active power transfer from the PV array to the grid. Figure 9(a) shows inverter currents for different solar irradiance and observes that inverter currents change accordingly. Figure 9(b) shows a dynamic change in grid current for a change in solar irradiance as PV power is directly supplying load/grid and also DC link voltage is maintained constant with PV power variation (PV power variation is achieved by covering the PV array with a semi transparent sheet). Only active filtering mode is shown in Figure 9(c) and Figure 9(d). Inverter current follows the reference current generated using proposed algorithm in Figure 9(c)

and in 9(d); its effect on grid current is shown. As is clear that after inverter current follows reference, the grid current becomes as PV inverter supplies required reactive power. Figures 9(e)-(f) shows hybrid mode in which active and reactive both powers are supplied by the PV inverter. PV power variation for the conditions like low load-high PV power as well as high load-low PV power is depicted in Figure 9(e). Figure 9(f) shows dynamic condition of all modes i.e., upto region 1, only real power is injected into grid, 2nd region shows condition where both real and reactive power is supplied by PV inverter and at 3rd region PV array is removed so now inverter will act as active filter only.

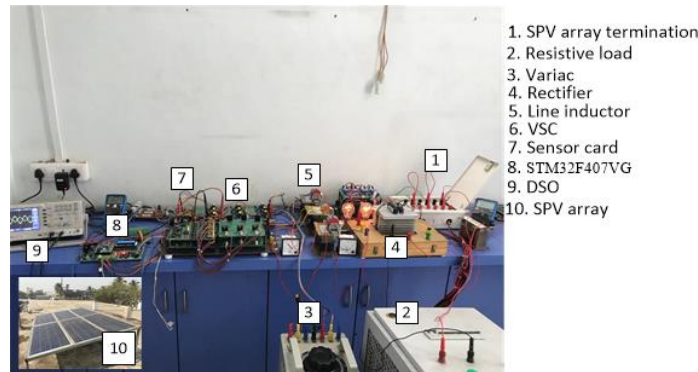


Figure 8. Hardware setup for proposed algorithm

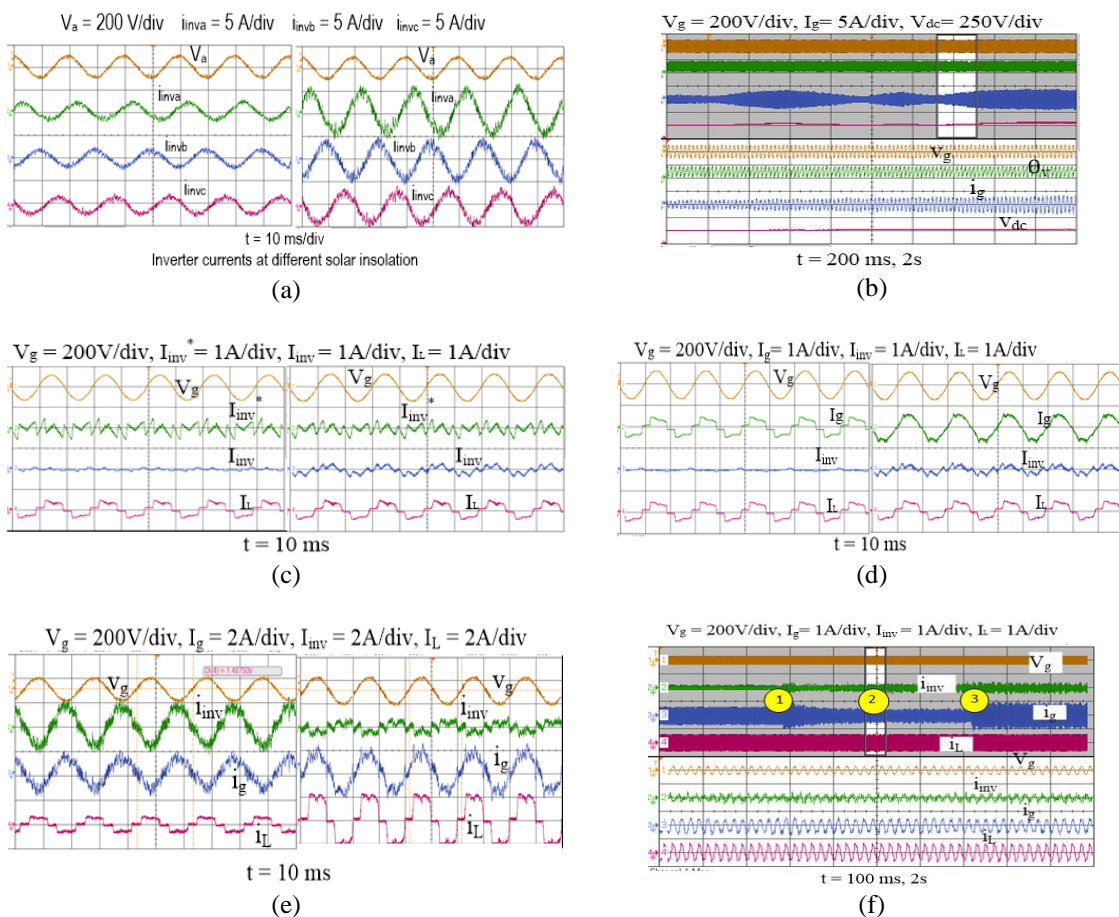


Figure 9. Experimental results under different modes (a) steady state performance for PV mode, (b) dynamic performance for PV mode, (c) active filter mode (inverter current), (d) active filter mode (grid current), (e) hybrid mode (steady state performance), and (f) hybrid mode (dynamic performance)

4. CONCLUSION

The proposed adaptive l_0 -LMS algorithm is implemented in the PV-DSTATCOM system for mitigation of various PQ issues. The proposed algorithm has been tested for conditions of load unbalancing and variable solar irradiance and the results are found satisfactory. The adaptive l_0 -LMS algorithm has the ability to adapt to time-varying signals as it generates proper control signals under varying load and atmospheric conditions. Zero attractor is added to the update equation of tap weight vector, which increases the convergence speed. From the results, it is also observed that the PQ of the system is maintained while it continues to supply maximum power extracted from PV array. Results are verified on low cost laboratory prototype developed using STM32F407VG microcontroller.

REFERENCES

- [1] R. K. Varma, V. Khadkikar, and R. Seethapathy, "Nighttime Application of PV Solar Farm as STATCOM to Regulate Grid Voltage," *IEEE Transactions on Energy Conversion*, vol. 24, no. 4, pp. 983–985, Dec. 2009, doi: 10.1109/tec.2009.2031814.
- [2] N. Femia, G. Petrone, G. Spagnuolo, and M. Vitelli, "A Technique for Improving P&O MPPT Performances of Double-Stage Grid-Connected Photovoltaic Systems," *IEEE Transactions on Industrial Electronics*, vol. 56, no. 11, pp. 4473–4482, Nov. 2009, doi: 10.1109/tie.2009.2029589.
- [3] M. A. G. de Brito, L. Galotto, L. P. Sampaio, G. de A. e Melo, and C. A. Canesin, "Evaluation of the Main MPPT Techniques for Photovoltaic Applications," *IEEE Transactions on Industrial Electronics*, vol. 60, no. 3, pp. 1156–1167, Mar. 2013, doi: 10.1109/tie.2012.2198036.
- [4] Q. Mei, M. Shan, L. Liu, and J. M. Guerrero, "A Novel Improved Variable Step-Size Incremental-Resistance MPPT Method for PV Systems," *IEEE Transactions on Industrial Electronics*, vol. 58, no. 6, pp. 2427–2434, Jun. 2011, doi: 10.1109/tie.2010.2064275.
- [5] M. Godavarti and A. O. Hero, "Partial update LMS algorithms," *IEEE Transactions on Signal Processing*, vol. 53, no. 7, pp. 2382–2399, Jul. 2005, doi: 10.1109/tsp.2005.849167.
- [6] A. K. Kohli and D. K. Mehra, "Tracking of time-varying channels using two-step LMS-type adaptive algorithm," *IEEE Transactions on Signal Processing*, vol. 54, no. 7, pp. 2606–2615, Jul. 2006, doi: 10.1109/tsp.2006.874779.
- [7] D. P. Das, S. R. Mohapatra, A. Routray, and T. K. Basu, "Filtered-s LMS algorithm for multichannel active control of nonlinear noise processes," *IEEE Transactions on Audio, Speech and Language Processing*, vol. 14, no. 5, pp. 1875–1880, Sep. 2006, doi: 10.1109/taus.2005.858543.
- [8] Y.-S. Choi, H.-C. Shin, and W.-J. Song, "Robust Regularization for Normalized LMS Algorithms," *IEEE Transactions on Circuits and Systems II: Express Briefs*, vol. 53, no. 8, pp. 627–631, Aug. 2006, doi: 10.1109/tcsii.2006.877280.
- [9] L. R. Vega, H. Rey, J. Benesty, and S. Tressens, "A Fast Robust Recursive Least-Squares Algorithm," *IEEE Transactions on Signal Processing*, vol. 57, no. 3, pp. 1209–1216, Mar. 2009, doi: 10.1109/tsp.2008.2010643.
- [10] K. Mayyas, "A variable step-size selective partial update LMS algorithm," *Digital Signal Processing*, vol. 23, no. 1, pp. 75–85, Jan. 2013, doi: 10.1016/j.dsp.2012.09.004.
- [11] D. P. Das, S. M. Kuo, and G. Panda, "New block filtered-X LMS algorithms for active noise control systems," *IET Signal Processing*, vol. 1, no. 2, pp. 73–81, Jun. 2007, doi: 10.1049/iet-spr:20060220.
- [12] A. K. Giri, S. R. Arya, and R. Maurya, "Compensation of Power Quality Problems in Wind-Based Renewable Energy System for Small Consumer as Isolated Loads," *IEEE Transactions on Industrial Electronics*, vol. 66, no. 11, pp. 9023–9031, Nov. 2019, doi: 10.1109/tie.2018.2873515.
- [13] A. K. Giri, S. R. Arya, R. Maurya, and R. Mehar, "Variable learning adaptive gradient based control algorithm for voltage source converter in distributed generation," *IET Renewable Power Generation*, vol. 12, no. 16, pp. 1883–1892, Oct. 2018, doi: 10.1049/iet-rpg.2018.5213.
- [14] A. K. Giri, S. R. Arya, R. Maurya, and B. C. Babu, "Mitigation of power quality problems in PMSG-based power generation system using quasi-Newton-based algorithm," *International Transactions on Electrical Energy Systems*, vol. 29, no. 11, Jul. 2019, doi: 10.1002/2050-7038.12102.
- [15] R. K. Agarwal, I. Hussain, and B. Singh, "Implementation of LLMF Control Algorithm for Three-Phase Grid-Tied SPV-DSTATCOM System," *IEEE Transactions on Industrial Electronics*, vol. 64, no. 9, pp. 7414–7424, Sep. 2017, doi: 10.1109/tie.2016.2630659.
- [16] T. Khan, M. Asim, M. S. Manzar, M. Ibrahim, and S. S. A. Ahmed, "Least mean sixth control approach for three-phase three-wire grid-integrated PV system," *International Journal of Power Electronics and Drive Systems (IJPEDS)*, vol. 12, no. 4, p. 2131, Dec. 2021, doi: 10.11591/ijpeds.v12.i4.pp2131-2139.
- [17] M. Ehtesham and M. Junaid, "Advanced compensation scheme for enhancing photovoltaic power quality," *Indonesian Journal of Electrical Engineering and Computer Science*, vol. 27, no. 3, p. 1223, Sep. 2022, doi: 10.11591/ijeecs.v27.i3.pp1223-1230.
- [18] K. Sudarsan and G. Sreenivasan, "PV solar farm as static synchronous compensator for power compensation in hybrid system using Harris Hawks optimizer technique," *International Journal of Power Electronics and Drive Systems (IJPEDS)*, vol. 13, no. 1, p. 554, Mar. 2022, doi: 10.11591/ijpeds.v13.i1.pp554-560.
- [19] K. Saleh and O. Mahmoud, "Asymmetrical four-wire cascaded h-bridge multi-level inverter based shunt active power filter supplied by a photovoltaic source," *International Journal of Power Electronics and Drive Systems (IJPEDS)*, vol. 12, no. 3, p. 1673, Sep. 2021, doi: 10.11591/ijpeds.v12.i3.pp1673-1686.
- [20] M. Kandpal, I. Hussain, and B. Singh, "ZA-QLMS based control approach for DSTATCOM under abnormal grid conditions," in *2016 IEEE 7th Power India International Conference (PIICON)*, Nov. 2016, doi: 10.1109/poweri.2016.8077258.
- [21] R. Faranda, S. Leva, and V. Maugeri, "MPPT techniques for PV Systems: Energetic and cost comparison," in *2008 IEEE Power and Energy Society General Meeting - Conversion and Delivery of Electrical Energy in the 21st Century*, Jul. 2008, doi: 10.1109/pes.2008.4596156.
- [22] R. A. Mastromauro, M. Liserre, and A. Dell'Aquila, "Control Issues in Single-Stage Photovoltaic Systems: MPPT, Current and Voltage Control," *IEEE Transactions on Industrial Informatics*, vol. 8, no. 2, pp. 241–254, May 2012, doi: 10.1109/tii.2012.2186973.
- [23] M. G. Villalva, J. R. Gazoli, and E. R. Filho, "Comprehensive Approach to Modeling and Simulation of Photovoltaic Arrays," *IEEE Transactions on Power Electronics*, vol. 24, no. 5, pp. 1198–1208, May 2009, doi: 10.1109/tpe.2009.2013862.

- [24] G. Su, J. Jin, Y. Gu, and J. Wang, "Performance Analysis of 10 Norm Constraint Least Mean Square Algorithm," *IEEE Transactions on Signal Processing*, vol. 60, no. 5, pp. 2223–2235, May 2012, doi: 10.1109/tsp.2012.2184537.
- [25] R. Yates and R. Lyons, "DC Blocker Algorithms [DSP Tips & Tricks]," *IEEE Signal Processing Magazine*, vol. 25, no. 2, pp. 132–134, Mar. 2008, doi: 10.1109/msp.2007.914713.

BIOGRAPHIES OF AUTHORS



Nimita A. Gajjar received the bachelor's degree in Electrical Engineering from Birla Vishwakarma Mahavidhyalaya in 1996. She received her M.Tech in Electrical Engineering with specialization in Industrial Electronics from SVNIT, Surat in 2009. Currently she is Associate Professor in Electrical Department of Government Engg. College, Surat under Gujarat Technological University, Gujarat, India. Her fields of interest include renewable energy, power quality and application of power electronics in distributed energy system. She can be contacted at email: nimita_gajjar@hotmail.com.



Dr. Tejas Zaveri is a former Associate Professor at the Department of Electrical Engineering, C.K.Pithawala college of engineering and technology, Surat. She has done B. Tech. in Electrical Engineering from SVNIT Surat, India, in 1999, and an M.E (Electrical) from MSU, Baroda in 2006. She has completed her Ph.D. in Electrical Engineering from VNSGU Surat, in 2012. Her research interests are in the area of power quality, power electronics, and custom power devices. where she has authored/co-authored many research publications. She can be contacted at email: tejas1009@gmail.com.



Dr. Naimish Zaveri is working as a Professor at the Department of Electrical Engineering, C.K. Pithawala college of engineering and technology, Surat. He did his B.Tech in Electrical Engineering from SVNIT Surat, India, in 1999, and obtained Masters degree (Electrical) from B. V. M. V. Nagar. He received his Ph.D. in Electrical Engineering from SVNIT Surat, in 2012. His research interests are primarily in the area of power quality, renewable energy, solar photovoltaic, and active filters. He can be contacted at email: naimish.zaveri@ckpcet.ac.in.